In: 2025 IEEE 7th International Conference on Computing, Communication and Automation (ICCCA), 28-30 November 2025, Greater Noida, India.
DOI: 10.1109/ICCCA66364.2025.11325136

A Novel LLM-AI Based Automation Framework for High Frequency Wireless Power Transfer Design

Khalifa Aliyu Ibrahim
Centre for Energy Engineering, Cranfield University
MK43 0AL, United Kingdom
Khalifa-Aliyu.Ibrahim@cranfield.ac.uk

Patrick Chi-Kwong Luk
Centre for Energy Engineering, Cranfield University
MK43 0AL, United Kingdom
p.c.k.luk@cranfield.ac.uk

Zhenhua Luo
Centre for Energy Engineering, Cranfield University
MK43 0AL, United Kingdom
Z.Luo@cranfield.ac.uk

Seng Yim Ng
SYNG Power Consulting Ltd, 78 High Street, Newport Pagnell, England, MK16 8AQ, United Kingdom
sengyim.ng@syngpowerconsultingltd.com

Lee Harrison
QBYSS LTD, Cranfield Technology Park, Unit 28/29 Innovation Centre,
MK43 0AL, United Kingdom
lee.harrison@QBYSS.com

***Abstract*— Designing high frequency wireless power transfer (WPT) systems typically involve complex modeling, simulation, and prototyping steps that demand significant time and expertise. In this study, we adopted and extended a previously proposed large language model (LLM) based design framework to accelerate design process. Seven customized generative pretrain transformers (GPT) based agents were developed using specific design guidance in WPT design to improve the accuracy of the generated outputs. A total of seven generated designs proposed by each agent were evaluated using the same design prompt. The generated designs were compared against four mathematical models based on design accuracy, completeness, and design time. The most accurate design was validated using PSIM and 3D Ansys simulation. The results demonstrate the potential of LLM-driven workflows to significantly reduce design effort and time while maintaining high reliability in WPT system development.**

Keywords*— *LLM-assisted design, Wireless power transfer, high frequency, artificial intelligence, power electronics, AI agents.

I. Introduction

Electrical systems remain a core component of global energy development and utilization [1]. The advancement of electrical systems is central to energy strategies, particularly in sectors requiring compact, efficient, and high performance power solutions. High frequency wireless power transfer (HFWPT) systems have gained traction as a viable technology for applications such as electric vehicles [2], [3], biomedical implants [4], and industrial automation where physical connectors are impractical or undesirable. These systems offer advantages including reduced system weight, minimized spatial footprint, and enhanced transmission efficiency. However, the conventional design process for power electronic (PE) systems, including HFWPT, remains highly complex, labor intensive, and time consuming [5], [6]. It typically spans multiple interdependent stages ranging from conceptual design and mathematical modeling to simulation, optimization, prototyping, and validation [7]. Each step demands precise engineering calculations and expert judgment, making the process vulnerable to human error and inefficiencies.

Streamlining design process can lead to significant reductions in development time and cost, while also improving the performance, reliability, and scalability of power systems. Recent efforts in power electronics research have leveraged computational tools and machine learning to support specific stages of the design process [8], [9], [10]. For example, some recent studies have applied neural networks for parameter optimization [11], while others have explored automatic circuit layout generation using machine learning [12]. However, a critical gap remains in the exploration of recent advancements in artificial intelligence (AI) particularly generative AI and large language models (LLMs).

Existing studies often overlook the potential of these models to deliver intelligent, contextual design support across the entire workflow. To address this gap, this paper adopted a novel framework based on LLM generative AI design introduce in our previous study as reported in [13]. The present work extends that framework through multi-agent benchmarking, and statistical validation. The wireless power transfer system (WPT) was entirely designed using an LLM-AI called High Frequency Power Electronic (HFPE-AI) specifically created 7 agents based on OpenAI's platform. We evaluate the design capabilities using a standardized prompt and compare the output with conventional mathematical modeling. The best designs were validated using Ansys 3-D finite element method (FEM) for the coil and PSIM simulation for system level performance. The key contributions of this paper are:

I. A quantitative benchmarking framework for evaluating LLM generated designs in terms of design time, accuracy and completeness.

II. A comprehensive comparative evaluation of seven fine tuned LLM agents (HFPE series) to assess prompt driven design robustness.

III. Proposed a two stage validation of LLM design process combining mathematical modeling and simulation.

The rest of the paper is organized as follows: Section II presents the proposed LLM driven design framework methodology. Section III describes the mathematical modeling and simulation setup. Section IV presents results and performance comparisons. Section V concludes the paper.

II. Proposed LLM Methodology

In this study, we refer to each of the HFPE-AI model version created such as 4o, o3, 4o-mini, 4o-mini-high, 4.5, 4.1, 4.1-mini as distinct "LLM agents," each representing a unique configuration of fine-tuned model capabilities, response behaviors, and computational efficiency. The proposed

framework utilizes various generative pretrain transformer GPT based agents to automate the entire design process of a WPT system as shown in Fig.1. Structured prompts were developed to sequentially guide the language model through tasks such as coil geometry specification, resonant circuit design, and component selection. The output generated was iteratively refined through prompt chaining until a complete design solution was achieved. This process enables rapid prototyping while minimizing human intervention, errors, and repetitive calculations. The framework bridges the gap between AI-generated natural language responses and practical engineering implementations. The LLM agent instructions structure and corresponding pseudocode are provided in the accompanying GitHub repository [14].

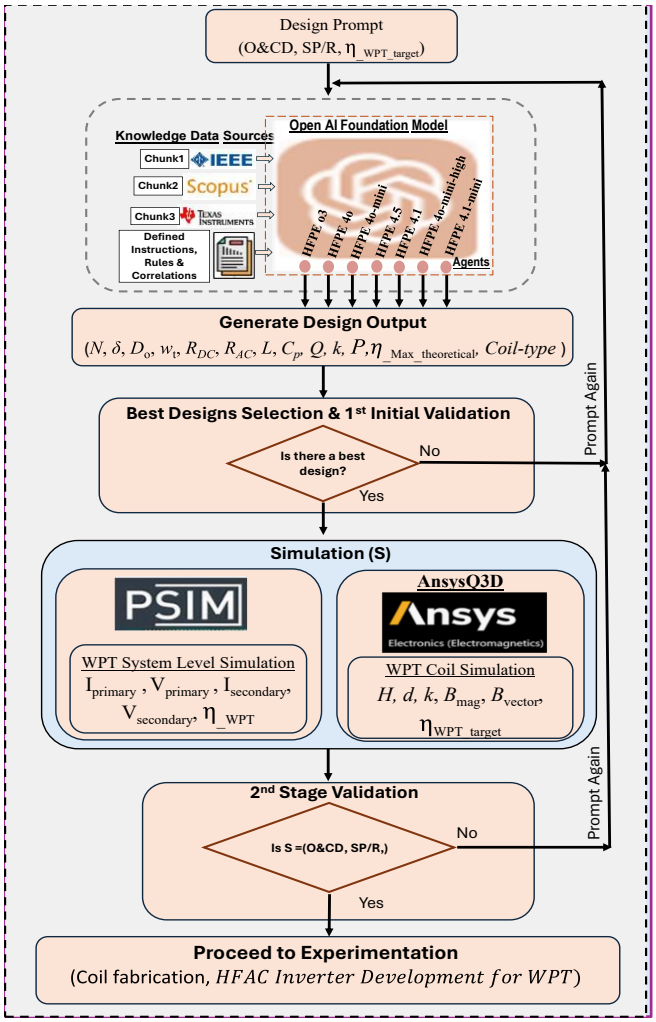

Fig. 1. Design workflow of LLMs AI for wireless power.

A. Prompt Engeneering Power Electronic Design Evaluation Metrics

To assess the effectiveness of the LLM generated designs, we proposed three core metrics which include design time, accuracy, and completeness. Design time saving (ΔT) was measured as the total duration from initial prompt input to generation of a proposed design ready for simulation or fabrication given by (1). Accuracy refers to how closely the LLM generated circuit parameters and coil specifications match validated conventional mathematical results which is a function of the absolute summation of the percentage difference ($\%\Delta$) as defined in (2). Completeness evaluates whether the design output includes all required design parameter for a working system. It quantifies how many of the AI-generated design outputs fall within an acceptable error margin of 5% compared to reference values. A higher completeness score indicates greater reliability and consistency in the AI's performance as defined in (3). These metrics allow for a quantitative and qualitative assessment of the LLM performance and its viability as a design assistant in power electronics. This reflects how consistently the AI method performs across a full design task.

$$Design\ time\ saving\ \Delta T = \left(1 - \frac{T_{AI}}{T_{Non-AI}}\right) \times 100 \quad (1)$$

$$Accuracy = 100\% - \left(\frac{\sum |\%\Delta|}{n}\right) \quad (2)$$

$$Completeness\ (\%) = \left(\frac{N_{within\ threshold}}{N_{total}}\right) \times 100\% \quad (3)$$

Where $N_{within\ threshold}$ is the number of predictions within the predefined accuracy threshold and N_{total} is the total number of predictions made. where T_{AI} is the time taken using the AI method and T_{Non-AI} is the time using conventional design methods. A higher ΔT indicates a more significant time saving benefit.

III. Modelling And Simulation

A. Mathematical Design of WPT

Conventional mathematical model of WPT system was developed to establish a performance. The model incorporates key equations to determine skin depth, resistance (DC and AC), inductance, parasitic and compensation capacitance, quality factor (Q), and maximum theoretical power transfer efficiency (η_{max}). These calculations used standard physical constants and assumed a flat spiral coil geometry operating at 85 kHz. The model served as a benchmark for evaluating the accuracy and validity of the LLM generated designs. A standard series-series compensated WPT system is illustrated in Fig. 2 (a). The components C_1, C_2 and L_1, L_2 are capacitors and coils inductance which are configured to achieve resonance, thereby enhancing power transfer efficiency. Assuming V represents the source voltage, and the $j\omega$ terms capture the reactive impedances of the primary and secondary circuits, as defined in (4) and (5), respectively. Fig. 2 (b) and (c) show the coil geometry and fabricated coil based on the best LLM-AI generated design. The fabricated coil confirmed the coil layout spatial alignment and shape.

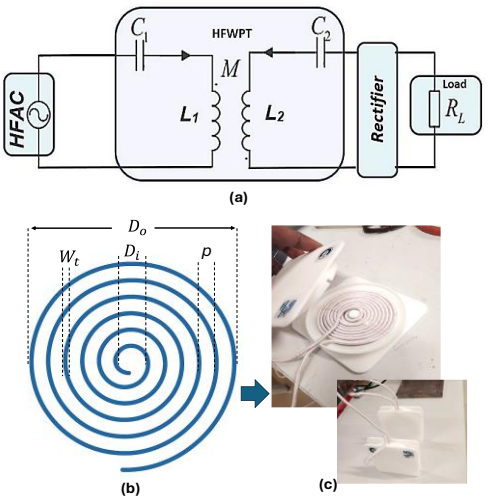

Fig. 2. (a) simplified circuit diagram of series-series HFWPT system (b) flat spiral coil geometry (c) fabricated coil.

$$V = (R_1 + R_s + j\omega L_1 + \frac{1}{j\omega C_1})I_1 + j\omega M I_2 \quad (4)$$

$$0 = (R_L + R_2 + j\omega L_2 + \frac{1}{j\omega C_2})I_2 + j\omega M I_1 \quad (5)$$

Where, R_s denotes the source resistance, while R_1 and R_2 represent the resistances in the primary and secondary circuits, respectively. R_L models the electrical load connected to the receiver. The currents I_1 and I_2 indicate the current flow in the primary and secondary circuits. At the resonant frequency, the inductive and capacitive reactance cancel each other, as described by (6) and (7), thereby minimizing reactive losses and maximizing power transfer efficiency.

$$V_s = (R_1 + R_s)I_1 + j\omega M I_2 \quad (6)$$

$$0 = (R_L + R_2)I_2 + j\omega M I_1 \quad (7)$$

The impedance of primary circuit coil and secondary circuit Z_2 is define by (8) and (9).

$$Z_1 = R_1 + R_s + j\omega L_1 + \frac{1}{j\omega C_1} \quad (8)$$

$$Z_2 = R_L + R_2 + j\omega L_2 + \frac{1}{j\omega C_2} \quad (9)$$

When (8) and (9) is substituted in (4) and (5) is simplified to (10) and (11). Solving for I_1 and I_2 using (12), (13), and (14) gives (15) and (16). The resonance frequency is given by (17).

$$V_s = Z_1 I_1 + j\omega M I_2 \quad (10)$$

$$0 = Z_2 I_2 + j\omega M I_1 \quad 11)$$

$$I_2 = -\frac{j\omega M I_1}{Z_2} \quad (12)$$

$$V_s = Z_1 I_1 + \frac{j\omega M(-j\omega M I_1)}{Z_2} \quad (13)$$

$$V_s = I_1\left(Z_1 + \frac{\omega^2 M^2}{Z_2}\right) \quad (14)$$

$$I_1 = \frac{V_s Z_2}{Z_1 Z_2 + \omega^2 M^2} \quad (15)$$

$$I_2 = -\frac{j\omega M V_s}{Z_1 Z_2 + \omega^2 M^2} \quad (16)$$

$$f_o = \frac{1}{2\pi\sqrt{L_o C_o}} \quad (17)$$

For a flat spiral coil geometry as shown in Fig. 2(b) with outer diameter D_o given by $D_o = D_i + 2N(w_t + p)$, inner diameter D_i, wire thickness w_t, pitch p and parasitic capacitance $C_p = 0.035D_o + 0.06$, the inductance is given by (18). The resonance capacitance C_o can be obtain with (17) if f_o is define. The coil DC resistance R_{DC}, and effective resistance R are given in (19). The Q factor and the maximum theoretical efficiency $\eta_{\max\_theoretical}$ are given by (20) and (21), respectively.

$$L_o = \frac{39.37\, N_o^2\, (D_o - N_o\,(w_t + p))^2}{16D_o + 28N_o\,(w_t + p)} \ [\mu H] \quad (18)$$

$$R = R_{DC}\frac{w_t}{4\delta}, \qquad R_{DC} = \frac{l}{\sigma\pi(w_t/2)^2}, \ \delta = \frac{1}{\sqrt{\pi f_s \sigma \mu_o}} \quad (19)$$

$$Q = \frac{\omega L_{eq}}{R_{eq}} = \frac{X_{eq}}{R_{eq}} = \frac{\omega(L - C_p R^2{}_o - C_p L^2 \omega^2}{R} \quad (20)$$

$$\eta_{\max\_theoretical} = \frac{k^2 Q_1 Q_2}{(1+\sqrt{1 + k^2 Q_1 Q_2})^2}, \text{ where } k = \frac{M}{\sqrt{L_1 L_2}} \quad (21)$$

B. *Simulation of LLM-Generated Designs*

To verify the LLM generated design, a circuit level simulations were performed using PSIM version 3.0.60-2022 due to its widely adoption in power electronics and resonant converter analysis. The primary objective was to confirm that the LLM-generated geometry could operate as expected when powered, providing a practical check of the AI-guided design pipeline. Seven different designs where generated, each design generated by each agent as shown in Table I. The best performing agent based on the evaluation metrics presented in section II was simulated.

The agent proposed a flat spiral geometry with 10 turns, a trace width of 3.5 mm, a pitch of 3.8 mm, and an outer diameter of approximately 82.5 mm to comply with a maximum total wire length of 1300 mm. For optimal performance at 85 kHz, the AI recommended a 450-strand Litz wire with individual strand diameters of 0.1 mm, selected to reduce skin effect losses. The simulated system architecture mirrored the AI-suggested parameters, including the number of turns, coil dimensions, Litz wire specifications, and compensation capacitance values. The objective was to validate the resonance behaviour, current and voltage waveforms, and power transfer efficiency at system level. ANSYS electronic version 2021 R2 was used to visualized and conduct electromagnetic field analysis. This study prioritised the end to end AI-driven design and its electrical performance based on the two simulation. However, the coil was fabricated as shown in Fig. 2 (c), directly based on the parameters generated by the best performing LLM agent.

IV. Results and Analysis

Table I presents a comprehensive comparison of multiple large language model (LLM) AI agents evaluated for their ability to design a wireless power transfer (WPT) system based on prompt driven outputs. The evaluation is categorized into three core metrics: response time (design time), accuracy deviation from validated models, and design completeness score. Among the tested models, HFPE-4o and its variants (4o-mini-high, and 4.1) demonstrated remarkable consistency in producing physically meaningful designs that closely match reference values obtained through mathematical modeling. Notably, HFPE-4o achieved a maximum theoretical efficiency (η_{max}) of 98.42% with negligible deviation in key parameters such as inductance (105.84µH), resistance (0.09 Ω), and resonance capacitance (33.12nF), while completing the design process in just 30 seconds representing a 99.17% reduction in time compared to conventional 1hour modeling.

In contrast, other agents such as HFPE-3.5 (o3) and 4.1-mini exhibited significant limitations, with one producing an unphysical coupling coefficient ($k \approx 0.00$) and another yielding an extreme quality factor ($Q \approx 15{,}453$) indicative of instability. While HFPE-4.5 offered extremely high theoretical performance (η_{max} = 99.58%), it introduced anomalies in other components like resonance capacitance and quality factor, suggesting potential issues with model balance. Design completeness scores further highlight the robustness of the newer HFPE-4o series, achieving up to 92.86% completeness compared to only 35.71% in some other variants. Overall, HFPE-4o and HFPE-4.1 demonstrated the most accurate, complete, and efficient design responses, making them strong candidates for AI-driven WPT system development in academic and industrial applications.

TABLE I. COMPARISON OF LLM -AI AGENTS BASED ON PROMPT RESPONSE TIME, ACCURACY DEVIATION, AND DESIGN COMPLETENESS SCORE.

		Mathematical Modelling of LLM-AI Proposed Design				WPT As Proposed by HFPE LLM-AI Driven Design													
Parameter	**Unit**	**Model 1 (4o, 4o-mini, 4o-mini-high, 4.1)**	**Model 2 (o3)**	**Model 3 (4.5)**	**Model 4 (4.1-mini)**	**HFPE 4o**	**%Δ**	**HFPE o3**	**%Δ**	**HFPE 4o-mini**	**%Δ**	**HFPE 4o-mini-high**	**%Δ**	**HFPE 4.5**	**%Δ**	**HFPE 4.1**	**%Δ**	**HFPE 4.1-mini**	**%Δ**
Skin Depth (δ)	mm	0.23	0.23	0.23	0.23	0.23	0.01	0.23	0.15	0.23	0.01	0.23	0.01	0.23	0.15	0.23	0.15	0.23	0.15
Number of Turns (N)	–	10.00	9.00	10.00	10.00	10.00	0.00	9.00	0.00	10.00	0.00	10.00	0.00	10.00	0.00	10.00	0.00	10.00	0.00
Outer Diameter (Do)	mm	82.51	76.00	114.40	77.90	82.51	0.00	76.00	0.00	82.51	0.00	82.51	0.00	114.40	0.00	82.50	-0.01	77.90	0.00
Trace Width (wt)	mm	3.50	3.50	3.50	3.50	3.50	0.00	3.50	0.00	3.50	0.00	3.50	0.00	3.50	0.00	3.50	0.00	3.50	0.00
Pitch Size (p)	mm	3.80	3.80	3.80	3.80	3.80	0.00	3.80	0.00	3.80	0.00	3.80	0.00	3.80	0.00	3.80	0.00	3.80	0.00
Wire Length (l)	mm	1300.00	1220.00	1300.00	1300.00	1300.00	0.00	1220.00	0.00	1300.00	0.00	1300.00	0.00	1300.00	0.00	528.00	-59.38	1300.00	0.00
Litz Wire Recommended	strands × mm	450 × 0.1	450 × 0.1	450 × 0.1	450 × 0.1	450 × 0.1	451 × 0.1	450 × 0.10	451 × 0.10	450 × 0.10	451 × 0.10	451 × 0.10	452 × 0.10	452 × 0.10	453 × 0.10	453 × 0.10	454 × 0.10	454 × 0.10	455 × 0.10
DC Resistance (RDC)	Ω	0.02	0.02	0.02	0.02	0.02	0.02	0.02	1.09	0.02	0.02	0.02	0.02	0.02	0.02	0.00	-95.94	0.00	-90.00
AC Resistance (R)	Ω	0.09	0.08	0.09	0.09	0.09	-0.03	0.09	1.19	0.09	-0.03	0.09	-0.03	0.09	-0.03	0.00	-95.94	0.01	-90.00
Inductance (L)	µH	105.84	110.72	1741.65	28.73	105.84	0.00	110.70	-0.02	105.84	0.00	105.84	0.00	1.74	-99.90	105.50	-0.32	28.50	-0.79
Parasitic Capacitance (Cp)	pF	2.95	2.72	4.06	2.79	2.95	0.07	2.72	0.00	2.95	0.07	2.95	0.07	0.06	-98.43	2.95	0.07	2.79	0.13
Resonance Capacitance (C)	nF	33.12	31.66	2.01	122.04	33.12	-0.01	31.70	0.11	33.12	-0.01	33.12	-0.01	2010.00	99752.13	33.20	0.23	123.00	0.79
Quality Factor (Q)	–	572.63	640.48	-10538.83	166.72	572.63	0.00	692.00	8.04	572.60	0.00	572.60	0.00	103.30	-100.98	15453.00	2598.62	1693.00	915.50
Coupling Coefficient (k)	–	0.20	1.74	0.04	0.00	0.20	0.01	0.20	-88.52	0.20	-0.04	0.20	-0.04	0.20	345.08	0.20	-0.04	0.20	Very high
Max theoretical Efficiency (η_{max})	%	98.42	99.82	99.58	0.00	98.42	0.00	98.60	-1.22	98.40	-0.02	98.42	0.00	90.00	-9.62	90.80	-7.74	99.41	Very high
Design Time	s	3600	3600	3600	3600	30		342		32		62		230		50		48	
Evaluation Metrics (Indicators)					Design Time save (%)	99.17		90.50		99.11		98.28		93.61		98.61		98.67	
					Accuracy	99.99		92.83		99.98		99.99		Very Low		Very Low		Very Low	
					Completeness	92.86		50.00		92.86		92.86		50.00		35.71		35.71	

Fig.3 presents the PSIM simulation results of the wireless power transfer (WPT) system designed using a Large Language Model (LLM) driven framework. The simulation displays time domain waveforms for the primary current I_{pri}, inverter output voltage V_{pri}, secondary current I_{sec}, and secondary voltage V_{sec}. The primary current waveform is sinusoidal and synchronized with the square wave inverter output, indicating that the system operates at its resonant frequency of 85 kHz. On the secondary side, the clean sinusoidal waveforms of both current and voltage confirm effective inductive coupling and minimal distortion. From the RMS values $V_{pri} = 59.96V$, I_{pri}= 4.22A, $V_{sec} = 47.71V$ and $I_{sec} = 4.77$A. The power transfer efficiency is calculated to be approximately 90.2%. This result validates the accuracy of the LLM generated coil and circuit parameters, demonstrating the potential of AI-assisted design methodologies for rapid and high-performance WPT system development.

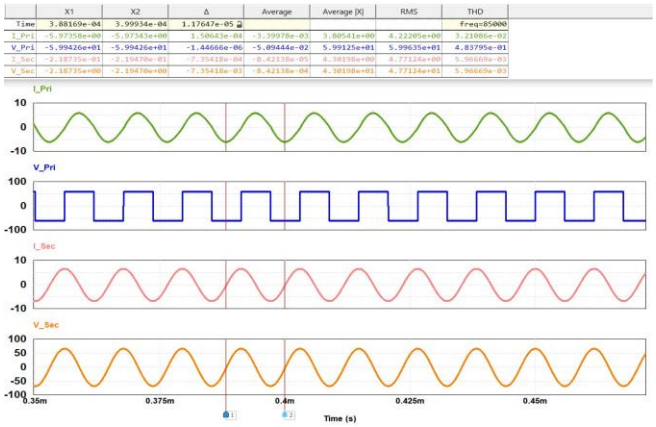

Fig. 3. PSIM simulation of of best proposed LLM-drven design WPT

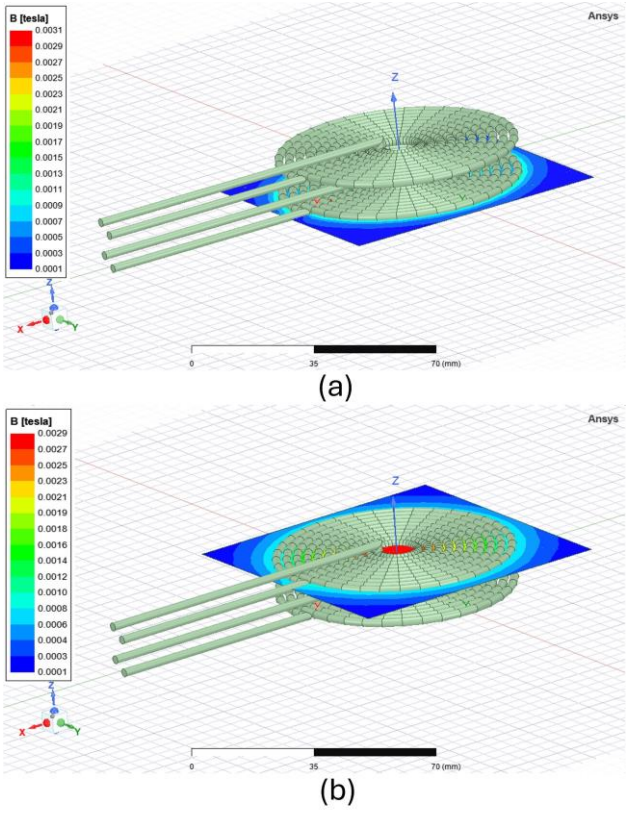

Fig. 4. Coil Ansys simulation of best proposed LLM-drven design WPT (a) field around primary coil (b) field around secondary coil

The electromagnetic field distribution was simulated using ANSYS Maxwell to evaluate the magnetic coupling performance of the LLM driven design. As shown in Fig. 4, the magnetic flux density contours around the primary and secondary coils confirm strong field confinement and symmetric along the coil axis. The flux distribution remains concentrated within the core coil region, ensuring efficient coupling. Furthermore, Fig. 5 illustrates the vector field intensity, with pronounced flux directionality and density between the coils highlighting a dominant vertical component in the z-axis and confirming high mutual inductance. These results support the field-focused design predicted by the LLM-based approach and validate its electromagnetic compatibility for high efficiency wireless power transfer.

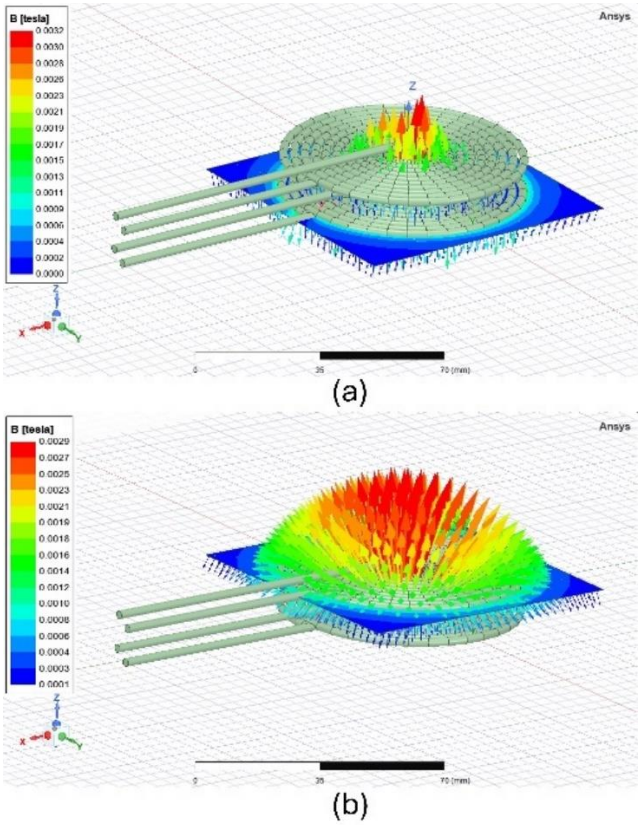

Fig. 5. Coil Ansys simulation of best proposed LLM-drven design WPT (a) field around primary coil (b) field around secondary coil

Fig. 6 illustrates the impact of coil separation on magnetic performance and transmission efficiency in the LLM-driven design. In Fig. 6 (a), both magnetic flux density at the receiver (Rx) and the corresponding magnetic field strength (H) decrease significantly as distance increases, while the transmitter (Tx) maintains a near-constant field. Fig. 6(b) correlates this decline in Rx flux with a rapid drop in wireless power transfer efficiency (η), confirming the sensitivity of coupling performance to coil alignment. The Tx flux remains unaffected, validating that performance degradation stems from weakened mutual inductance, not source instability. These results underscore the importance of precise coil positioning in practical deployment of LLM-designed WPT systems. The HFPE-4o design achieves 98.42% theoretical efficiency, with PSIM confirming 90.2% and ANSYS showing 90.6% efficiency at 2 mm separation; the small deviation from theory is attributed to model limitations and unmodelled parasitic effects.

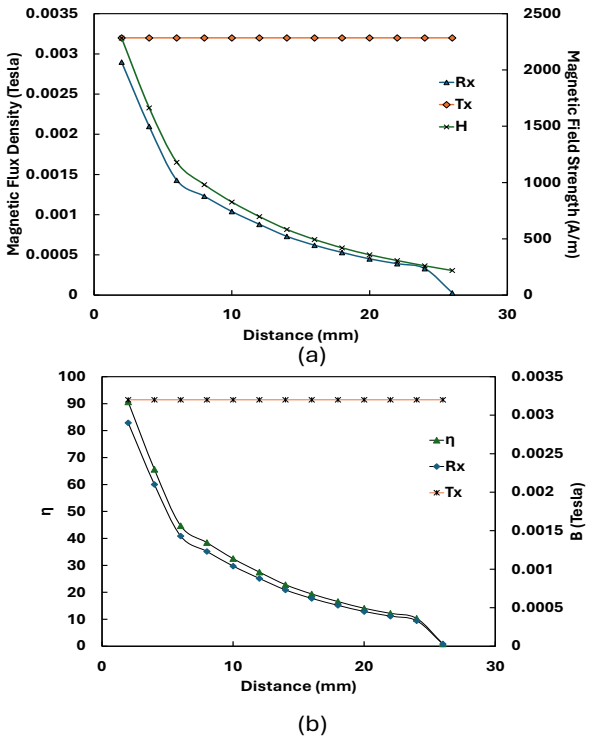

Fig. 6. Magnetic and efficiency response of the LLM-driven WPT coil design versus distance: (a) Magnetic flux density and field strength variation; (b) Impact of coil separation on transmission efficiency and receiver magnetic flux.

Fig. 7 the performance of seven LLM agents based on the proposed evaluation metrics. Each of the fine tuned LLM agents (HFPE series) exhibit clear performance variations across the proposed evaluation metrics. The HFPE-4o and HFPE-4o-mini-high agents demonstrate superior accuracy and completeness, while HFPE-4.5 and HFPE-4.1 show lower accuracy despite high time-saving values. This variability reflects the dependence of model performance on prompt formulation and internal fine-tuning configuration. The comparative variations across agents further highlight the influence of prompt structure and fine tuning strategy on design quality and reproducibility. Together with (1) to (3), this figure provides statistical and empirical evidence of the framework's stability and design robustness.

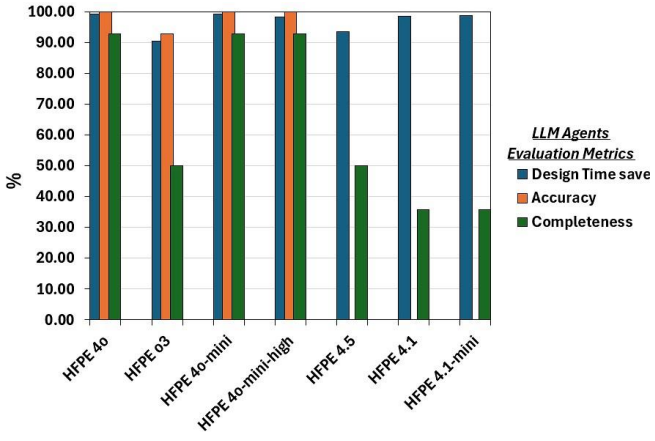

Fig. 7. Performance comparison of seven LLM agents based on the proposed evaluation metrics.

While the proposed LLM-AI framework demonstrates high efficiency and rapid design generation, it remains partially dependent on knowledge data, fine tune instructions, prompt structure and contextual grounding. The LLM generated coil parameters were directly implemented in PSIM and ANSYS to verify circuit and field-level responses. This cross validation links the AI-produced theoretical design with physical simulation domains, ensuring functional correlation before any experimental stage. Occasional model hallucinations, such as unrealistic or incomplete parameter suggestions, were mitigated through a two-stage validation process incorporating mathematical modeling, simulation based checks, and the three proposed evaluation metrics (design time, accuracy, and completeness).

Whereas this study focuses on wireless power transfer (WPT) systems, the underlying concept of LLM-driven generative design aligns with broader AI-assisted automation trends observed in circuit optimization, mechanical CAD design, and system-level digital twin development. Similar frameworks have been reported in domains such as control co-design and topology optimization, demonstrating that the integration of generative AI and engineering constraints is a growing multidisciplinary direction.

V. Conclusion

This study presents an AI-driven design framework for wireless power transfer (WPT) systems using large language models (LLMs). By prompting seven distinct LLM agents with unified design instructions, the framework rapidly generates complete coil and circuit designs, including geometry, compensation topology, and Litz wire specifications. The best performing agent produces a fully detailed WPT design in under 60 seconds, achieving 99.17% design time savings, 99.99% accuracy, and 92.86% completeness, while maintaining engineering feasibility. PSIM circuit-level simulations verify the AI-generated designs with a power transfer efficiency of 90.2% based on RMS voltage and current values. ANSYS electromagnetic field simulations of the best design reveal strong magnetic coupling with a peak flux density of 0.0325 T and a maximum coupling efficiency of 90.625% at 2mm separation, confirming the coil layout's spatial alignment and magnetic effectiveness. Compared to traditional iterative methods, the LLM assisted process significantly reduces development time and removes multiple trial and error cycles.

Although physical testing is not part of this study, it forms a core component of future work. Planned developments include experimental validation of the AI-generated coil using a high frequency inverter, as well as the integration of thermal considerations into the design loop. Future research also leverages large scale, validated power-electronics datasets to train and fine tune LLMs for higher accuracy, adaptability, and domain specific reasoning. Coupling LLM agents with simulation feedback, symbolic solvers, and physics informed neural networks (PINNs) further strengthens predictive capability and reliability. Overall, this research demonstrates the transformative potential of generative AI to co-design and accelerate innovation in power electronics.

VI. Funding

This work is funded by QBYSS (Formerly Energy Research Lab (ERL)) and Cranfield University.

VII. References

[1] F. Salomez *et al.*, "State of the Art of Research towards Sustainable Power Electronics," *Sustainability*, vol. 16, no. 5, p. 2221, Mar. 2024, doi: 10.3390/su16052221.

[2] P. S. Subudhi and S. Krithiga, "Wireless Power Transfer Topologies used for Static and Dynamic Charging of EV Battery: A Review," 2020. doi: 10.1515/ijeeps-2019-0151.

[3] R. Qin, J. Li, J. Sun, and D. Costinett, "Shielding Design for High-Frequency Wireless Power Transfer System for EV Charging With Self-Resonant Coils," *IEEE Trans Power Electron*, vol. 38, no. 6, 2023, doi: 10.1109/TPEL.2023.3251990.

[4] S. R. Khan, S. K. Pavuluri, G. Cummins, and M. P. Y. Desmulliez, "Wireless power transfer techniques for implantable medical devices: A review," 2020. doi: 10.3390/s20123487.

[5] T. Lagier *et al.*, "How Good are the Design Tools in Power Electronics?," in *2020 22nd European Conference on Power Electronics and Applications (EPE'20 ECCE Europe)*, IEEE, Sep. 2020, p. P.1-P.12. doi: 10.23919/EPE20ECCEEurope43536.2020.9215942.

[6] J. Jose, J. P. Therattil, T. Jarin, B. Deepanraj, and M. Sumbwanyambe, "Intelligent Circuit Optimization for a Wireless Power Transfer System Based on L2CL-LCL Compensation," in *International Conference on Distributed Computing and Optimization Techniques, ICDCOT 2024*, Institute of Electrical and Electronics Engineers Inc., 2024. doi: 10.1109/ICDCOT61034.2024.10515425.

[7] S. S. H. Rafin, H. Hussein, and O. A. Mohammed, "An Introduction to Power Electronics Design Methodology," in *2023 IEEE Design Methodologies Conference, DMC 2023*, 2023. doi: 10.1109/DMC58182.2023.10412603.

[8] T. Tigerprints and Y. Li, "VIRTUAL PROTOTYPING OF PEBB BASED POWER ELECTRONICS VIRTUAL PROTOTYPING OF PEBB BASED POWER ELECTRONICS SYSTEM FOR GROUND VEHICLES SYSTEM FOR GROUND VEHICLES," Clemson University, Clemson, South Calrolina, 2023. Accessed: May 29, 2024. [Online]. Available: https://tigerprints.clemson.edu/cgi/viewcontent.cgi?article=5120&context=all_theses

[9] N. Mariun, B. Omrane, I. Aris, S. Mahmoud, and T. Soib, "Power electronics design aid system, a knowledge-based approach," in *Proceedings of the International Conference on Power Electronics and Drive Systems*, 2003. doi: 10.1109/PEDS.2003.1283112.

[10] M. Petkovski and M. Kostov, "Model Based Design and Hardware in the Loop Testing in Power Electronics Courses," *TEM Journal*, vol. 1, no. 4, pp. 292–296, 2012, Accessed: May 29, 2024. [Online]. Available: https://eprints.uklo.edu.mk/id/eprint/1322

[11] T. Dragicevic, P. Wheeler, and F. Blaabjerg, "Artificial Intelligence Aided Automated Design for Reliability of Power Electronic Systems," *IEEE Trans Power Electron*, vol. 34, no. 8, pp. 7161–7171, Aug. 2019, doi: 10.1109/TPEL.2018.2883947.

[12] A. K. Khamis and M. Agamy, "Converter Circuits to Machine Learning: Optimal Feature Selection," in *2022 IEEE Energy Conversion Congress and Exposition, ECCE 2022*, 2022. doi: 10.1109/ECCE50734.2022.9947826.

[13] K. A. Ibrahim, P. C.-K. Luk, Z. Luo, S. Y. Ng, and L. Harrison, "Revolutionizing power electronics design through large language models: Applications and future directions," *Computers and Electrical Engineering*, vol. 123, p. 110248, Apr. 2025, doi: 10.1016/j.compeleceng.2025.110248.

[14] K. A. Ibrahim, P. C.-K. Luk, Z. Luo, S. Y. Ng, and L. Harrison, *LLM-WPT-Design-Workflow (Pseudocode Code Repository)*, GitHub, 2025. Available: https://github.com/Khalifa44432/LLM-WPT-Design-Workflow

A novel LLM-AI based automation framework for high frequency wireless power transfer design

Ibrahim, Khalifa Aliyu

2025-11-28

Ibrahim KA, Luk PC-K, Lu Z, et al., (2025) A novel LLM-AI based automation framework for high frequency wireless power transfer design. In: Proceedings of the 2025 IEEE 7th International Conference on Computing, Communication and Automation (ICCCA), 28-30 Nov 2025, Greater Noida, India

https://doi.org/10.1109/iccca66364.2025.11325136